

# Intramolecular Energy Transfer in a Covalently Linked Copper(II) Porphyrin–Free Base Porphyrin Dimer: Novel Spin Polarization in the Energy Acceptor

Motoko Asano-Someda,<sup>\*,†</sup> Art van der Est,<sup>\*,‡,§</sup> Uwe Krüger,<sup>‡</sup> Dietmar Stehlik,<sup>‡</sup>  
Youkoh Kaizu,<sup>†</sup> and Haim Levanon<sup>||</sup>

Department of Chemistry, Tokyo Institute of Technology, O-okayama, Meguro-ku, Tokyo, 152-8551, Japan,  
Fachbereich Physik, Freie Universität Berlin, Arnimallee 14, 14195 Berlin, Germany, and Department of  
Physical Chemistry, The Hebrew University of Jerusalem, Givat-Ram, Jerusalem 91904, Israel

Received: April 14, 1999; In Final Form: June 28, 1999

The excitation wavelength dependence of time-resolved EPR is used to demonstrate the pathway of intramolecular energy transfer in a covalently linked copper(II)–free base porphyrin dimer. Spin polarized spectra are presented for selective excitation of both the copper(II) porphyrin donor (at 540 nm) and the free base porphyrin acceptor (at 640 nm) at 50 and 80 K. In all cases the observed spectra are assigned to the triplet state of the free base which is coupled weakly to the copper ground state doublet. The polarization pattern generated by selective excitation of the free base half is indicative of intersystem crossing (ISC), whereas excitation of the copper(II) half gives an eaa/eea polarization pattern. The latter is rationalized in terms of energy transfer via the lowest excited trip–quartet state of the copper(II) moiety, followed by selective depopulation from the spin states with doublet character in the weakly coupled free base triplet–copper doublet system. This leads to a spectrum which resembles that of the free base triplet state with overpopulation of the  $T_{+1}$  and  $T_{-1}$  sublevels. The spin-selective electronic relaxation is supported by the fact that the rise time of the polarization is consistent with the decay rate of the triplet signal generated via ISC following direct excitation of the free base. Superimposed on these triplet spectra is a narrow emissive feature at  $g = 2.02$  and a very broad a/e pattern, both of which decay with the same rate. In addition, a short-lived absorptive feature at  $g = 2.00$  is observed at temperatures below 50 K. From their  $g$ -values and temperature dependence these features are tentatively assigned to quartet and doublet states in conformations of the complex in which the coupling between the free base triplet and Cu(II) ground state is strong.

## 1. Introduction

Long-range intramolecular energy transfer is of increasing interest, especially in ensembles which absorb visible light, because it is crucial to understanding photoharvesting systems in natural organisms as well as for utilizing solar energy and designing molecular photonic devices. A great many kinds of porphyrin dimers and oligomers, which can be exploited for this purpose, have been synthesized and studied extensively over the past decade.<sup>1</sup> In these covalently and noncovalently linked porphyrin systems, the interactions between the chromophores and intramolecular processes such as energy and electron transfer have been investigated<sup>1–20</sup> and discussed in terms of through-space and through-bond mechanisms.<sup>21–23</sup> In chemically bridged porphyrin dimers, the interaction between the two halves varies with the spacer unit, which not only can control their mutual distance and orientation but also can specify the nature of the intervening chemical bonds.<sup>1–6</sup> In particular, hybrid porphyrin dimers having two different central metal ions serve as excellent donor–acceptor systems, since the two halves have different excitation energies and redox potentials.<sup>4–19</sup> Moreover, the central metal ion of the macrocycle can sometimes change

the excited-state dynamics drastically. Thus, by varying the two metals, a variety of photophysical processes can be studied in a given complex.

It is well-known that zinc(II) porphyrin–free base porphyrin dimers undergo singlet–singlet energy transfer and that the rate depends on the distance, orientation, and linkage between the two halves.<sup>4–10</sup> In contrast to the large number of studies on the diamagnetic zinc(II)–free base dimers, relatively little attention has been paid to dimers involving paramagnetic metal ions.<sup>11–17</sup> This is primarily because most paramagnetic metalloporphyrins have ( $d, d^*$ ) or charge transfer excited states below their ( $\pi, \pi^*$ ) excited states, and the presence of these low-lying states involving the metal excitation accelerates deactivation immediately after energy transfer, or directly prohibits energy transfer itself.

Copper(II) porphyrin has an unpaired electron in a copper  $d_{\sigma}$  orbital, which has exchange interaction with the porphyrin  $\pi$ -electrons. This exchange interaction splits the porphyrin triplet states into so-called “trip–doublet” ( $^2T$ ) and “trip–quartet” ( $^4T$ ) states with an energy gap of several hundreds  $\text{cm}^{-1}$ ,<sup>24–30</sup> whereas the singlet states become “sing–doublet”  $^2S$  states. The nonzero exchange interaction also gives rise to the configuration interaction between the  $^2S_1$  and  $^2T_1$  states, thus yielding very fast intersystem crossing (ISC) of the porphyrin  $\pi$ -system, with a rate estimated as  $k_{\text{isc}} > (8 \text{ ps})^{-1}$ .<sup>31,32</sup> Therefore, the excitation to the  $^2S_1$  state leads to primary population of the  $^4T_1$  state following the prompt ISC and relaxation from the  $^2T_1$  to  $^4T_1$

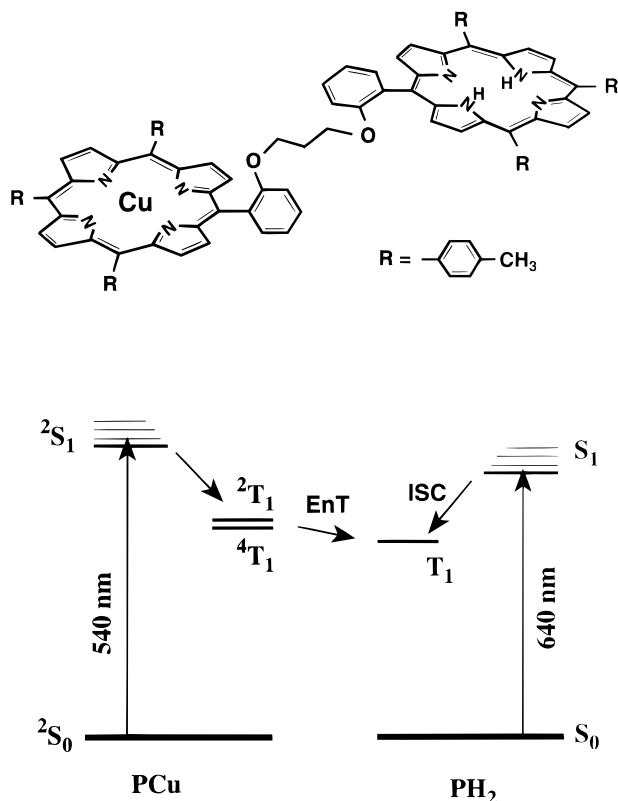
\* Corresponding author. E-mail: motoko@chem.titech.ac.jp. Fax: +81-3-5734-2655. E-mail: avde@brocku.ca. Fax: 1-905-688-2789.

<sup>†</sup> Tokyo Institute of Technology.

<sup>‡</sup> Freie Universität Berlin.

<sup>§</sup> Present address: Department of Chemistry, Brock University, 500 Glenridge Ave., St. Catharines Ont., Canada L2S 3A1.

<sup>||</sup> The Hebrew University of Jerusalem.

**SCHEME 1 Molecular Structure of Cu–C<sub>3</sub>–H<sub>2</sub> and an Energy Diagram of the Dimer Constituents**


states. In noncoordinating solvents, the  $^4T_1$  state is the lowest excited state,<sup>25–30</sup> because the (d, d<sup>\*</sup>) and charge transfer states are absent below the  $^2T_1$  and  $^4T_1$  states due to the strong ligand field and the d<sup>9</sup> configuration.

The lowest singlet and triplet excited states of the free base porphyrin are lower than the corresponding excited states of copper(II) porphyrin.<sup>33</sup> Therefore, intramolecular energy transfer from copper porphyrin to the free base can be expected in copper porphyrin–free base porphyrin hetero dimers. However, the rapid ISC process in the copper porphyrin moiety prevents energy transfer between the excited states of singlet ( $\pi, \pi^*$ ) character but allows energy transfer from the lowest excited states of the copper(II) porphyrin to the free base triplet state.<sup>12</sup>

Time-resolved EPR (TREPR) is well suited for studying such processes involving paramagnetic intermediates because the light-induced spin polarization patterns can be used to identify the states present in a given time window. Although the time resolution of the method is limited to  $\sim 10$  ns and diamagnetic species are not accessible, it is often possible to deduce the nature of short-lived precursor states based on their influence on the observed spectra. This is one of the most advantageous aspects of this method, wherein the resultant spectrum depends on the pathway by which the paramagnetic species is generated even in the condensed media. This is different from optical absorption measurements, which usually provide rather broad, pathway-independent spectra in such media due to fast vibrational relaxation within the electronic states.

Recently, we have used TREPR to study energy transfer in a copper(II)–free base porphyrin dimer with a three-carbon alkyl linkage.<sup>16</sup> Scheme 1 shows the structure of the dimer (Cu–C<sub>3</sub>–H<sub>2</sub>) and an energy diagram. Transient absorption measurements of the dimer suggested efficient intramolecular energy transfer via the trip–doublet and/or trip–quartet states of the Cu(II) half.<sup>12</sup> However, the rise of the acceptor could not be

observed because the transient absorption spectra of the two halves overlap severely. In this context, TREPR was expected to provide direct evidence of energy transfer to the triplet state of the free base. It was shown that selective excitation of the copper moiety at 532 nm and 77 K gave rise to a triplet-like spectrum with zero-field splitting (ZFS) parameters, characteristic of the free base but with an unusual polarization pattern. This spectrum was assigned to a triplet excitation of the free base in conformations of the dimer in which the coupling between the triplet and the copper doublet is weak. The observed polarization pattern suggests that the triplet state is not generated by ISC in the free base, and thus it is likely to be generated by intramolecular energy transfer. Nevertheless, the mechanism which yields this polarization pattern is not fully clarified. In addition, a narrow emissive signal at  $g \approx 2$ , which cannot be attributed to a triplet state, was also observed.

In the present study, we examine the excitation wavelength dependence of the TREPR spectra along with their temperature and orientation dependence, to investigate why photodynamics involving intramolecular energy transfer in this dimer leads to the unusual polarization pattern. We will clarify the origin of the polarization patterns by considering possible pathways and by presenting a mechanism which accounts for photophysical processes in the dimer. This report presents a novel observation that the energy acceptor has  $T_{+1}$  and  $T_{-1}$  overpopulation, which had been observed only for electron transfer cases.

**2. Experimental Section**

The free base–copper hybrid dimer Cu–C<sub>3</sub>–H<sub>2</sub> (Cu–C<sub>3</sub>–H<sub>2</sub> denotes [5-[2-[3-[2-[10,15,20-tris(4-methylphenyl)-21H,23H-porphyrin-5-yl]phenoxy]propoxy]phenyl]-10,15,20-tris(4-methylphenyl)porphyrinato]copper(II)-N,<sup>21</sup>N,<sup>22</sup>N,<sup>23</sup>N<sup>24</sup>) was synthesized as described previously.<sup>12,16</sup> EPR samples were prepared by dissolving the dimer in toluene (Merck, spectroscopic grade) or a liquid crystal, E7 (BDH) to give a final concentration of  $10^{-4}$  M. The solutions in Suprasil tubes (3 mm o.d.) were degassed by several freeze–pump–thaw cycles and then sealed under vacuum.

For the measurements in the liquid crystal (LC), macroscopic ordering in the solid phase of the sample was obtained by freezing from the nematic phase in the presence of the external magnetic field. Once frozen, the director of the LC was then rotated with respect to the magnetic field to give a desired orientation between the director and the field.

TREPR measurements were performed using a transient X-band microwave bridge (Bruker ER 046 XK-T) equipped with a dielectric resonator (Bruker model ER4118X-MD5(W1), unloaded  $Q = 4000$ ). The time resolution of the spectrometer with diode detection and a narrow band amplifier is estimated as  $\tau(1/e) = 500$  ns. The sample temperature was controlled in a helium gas-flow cryostat (Oxford CF935). A microwave power of 0.08 mW was used for all the measurements. The sample was excited using an optical parametric oscillator (Quanta-Ray MOPO-710) pumped by a frequency tripled Nd:YAG laser (Quanta-Ray GCR-170). The wavelength accuracy of the system is 5 nm, and a pulse energy of  $\sim 2$  mJ was used. The output power variation of the laser is less than 10% between 450 and 680 nm. The wavelength of the laser can be changed easily by rotating a BBO crystal in the oscillator without changing other conditions, and this allows for reliable wavelength-dependent measurements on the same sample.

The time development of the EPR absorption signal was digitized using a transient recorder (LeCroy 9350A) which was triggered by the laser flash. Transients were collected at a series of equally spaced magnetic field positions over a given range

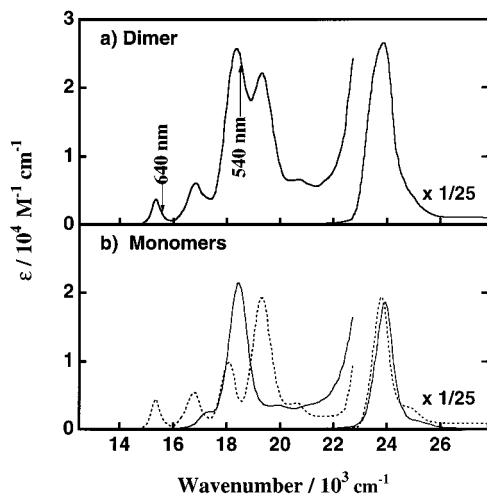


**Figure 1.** Absorption spectra of (a) Cu-C<sub>3</sub>-H<sub>2</sub> dimer and (b) porphyrin monomers, TTPCu (—) and TTPH<sub>2</sub> (---), in toluene at room temperature.

and transferred to a computer. Spectra are generated from the time/field data set by numerically integrating over an appropriate time window and subtracting the average baseline before the trigger event.

### 3. Results

**3.1. Excitation Wavelength Dependence at 80 K.** Figure 1 shows the optical absorption spectra of the dimer Cu-C<sub>3</sub>-H<sub>2</sub> and the monomers TTPH<sub>2</sub> (TTP: 5,10,15,20-tetratolylporphyrin) and TTPCu in toluene at room temperature. Since the absorption Q-band of the dimer is approximately described as a 1:1 superposition of those of the two monomers, the transitions to the S<sub>1</sub> states of both halves can be considered as independent. As can be seen in Figure 1, the free base monomer has an absorption at 640 nm, which is absent in the Cu(II) monomer. Similarly, the absorption intensity of the copper porphyrin at 540 nm is strong while that of the free base is weak. As a result, it is possible to selectively excite the two halves in the dimer with these wavelengths.

*Selective Excitation of the Free Base Half.* Figure 2 shows TREPR spectra of Cu-C<sub>3</sub>-H<sub>2</sub> in toluene with selective irradiation of the free base half ( $\lambda_{\text{ex}} = 640 \text{ nm}$ ,  $T = 80 \text{ K}$ ). The spectrum taken in the time window 0.8–1.2  $\mu\text{s}$  after the laser flash (top) is very similar to that of the triplet state of the corresponding free base monomer formed by ISC. This indicates that (i) in terms of the selectivity of the population into the triplet sublevels, ISC within the free base half is not affected by the copper porphyrin counterpart and (ii) the ZFS parameters of the free base half are almost identical to those of the monomer. However, some differences associated with the signal decay are observed.

As seen from the time development of the EPR spectra of the dimer (Figure 2), the features associated with the X-canonical orientation decay more rapidly than those associated with the Y and Z orientations. The decay profiles taken at field positions corresponding to the X orientation (not shown) exhibit a major component (>90%) with  $\tau \approx 2 \mu\text{s}$  and a minor component with  $\tau \approx 20 \mu\text{s}$ . In the case of the monomer, the features from the X orientation decay more slowly and show two kinetic phases of equal intensity governed by  $\tau \approx 5 \mu\text{s}$  and  $\tau \approx 30 \mu\text{s}$ . By contrast, the intensities for the Z orientation decay with much the same time constant in the monomer ( $\tau \approx 14 \mu\text{s}$ ) and dimer ( $\tau \approx 11 \mu\text{s}$ ). Another difference is the existence of a weak, broad

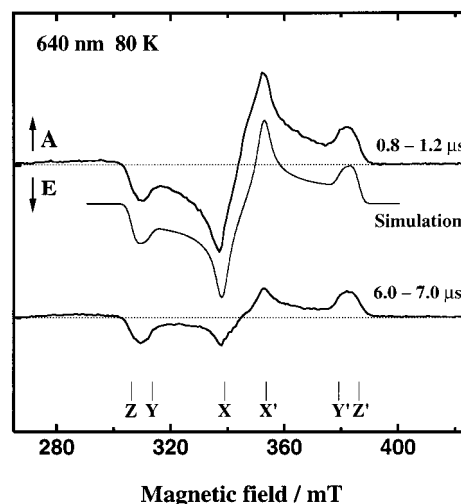


**Figure 2.** TREPR spectra of Cu-C<sub>3</sub>-H<sub>2</sub> in toluene excited at 640 nm and 80 K. Upper spectrum: detection gate time is 0.8–1.2  $\mu\text{s}$  following the laser pulse. Lower spectrum: detection gate 6.0–7.0  $\mu\text{s}$ . The intensities of the spectra are normalized to account for the different gate widths. Middle spectrum: simulation using parameters typical of the free base monomer. ZFS parameters:  $D = 375 \times 10^{-4} \text{ cm}^{-1}$ ;  $E = 80 \times 10^{-4} \text{ cm}^{-1}$ . Initial population ratio:  $P_x/P_y/P_z = 0.75:0.25:0$ . Line width:  $\Delta B = 2.0 \text{ mT}$ . The corresponding values for the monomer, TTPH<sub>2</sub> in ref 16 are  $D = 372 \times 10^{-4} \text{ cm}^{-1}$ ,  $E = 79 \times 10^{-4} \text{ cm}^{-1}$ ,  $P_x/P_y/P_z = 0.72:0.28:0$ , and  $\Delta B = 1.0 \text{ mT}$ . Arrows A and E stand for microwave absorption and emission, respectively.

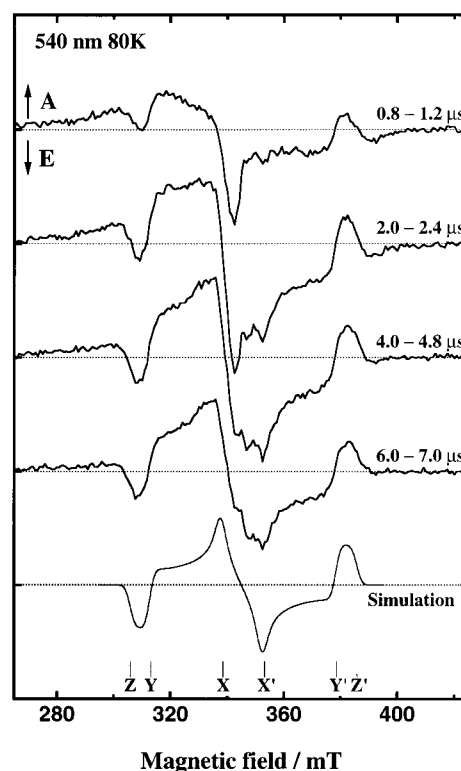


**Figure 3.** Time development of TREPR spectra of Cu-C<sub>3</sub>-H<sub>2</sub> in toluene excited at 540 nm and 80 K, together with a simulated spectrum (bottom). The detection gate times after the laser pulse from top to bottom are 0.8–1.2, 2.0–2.4, 4.0–4.8, and 6.0–7.0  $\mu\text{s}$ , respectively. For the simulation, a population ratio  $(T_{+1} - T_0)/(T_{-1} - T_0) = 0.5:0.5$  is used. Other details are the same as for Figure 2.

absorptive feature on the low-field side of the dimer spectrum, which is not observed in the monomer.

*Selective Excitation of the Copper Half.* Figure 3 shows TREPR spectra obtained with selective excitation of the copper

half of the dimer ( $\lambda_{\text{ex}} = 540$  nm, 80 K). In contrast to the copper monomer, which gives no spin-polarized TREPR signal between 20 and 300 K,<sup>16,17</sup> the spectra of the dimer in Figure 3 show two main components. One is a spectrum which is characterized by the same ZFS parameters as the triplet state of the free base monomer and which is seen most clearly in the time window 6.0–7.0  $\mu\text{s}$  (see Figure 3). The polarization pattern from low to high magnetic field is eaa/eea, where e stands for microwave emission and a stands for absorption. We assign the spectrum to the triplet state of the free base half of the dimer weakly coupled to the Cu(II) ground state and refer to it as the “triplet component”. The other component is a narrow, emissive feature at  $g = 2.02$  (see Figure 3, top trace).

The eaa/eea polarization pattern of the triplet component is different from that obtained when the free base is selectively excited. As described in the Experimental Section, the measurements with  $\lambda_{\text{ex}} = 540$  nm were done just before or after the measurements with  $\lambda_{\text{ex}} = 640$  nm on the same sample. Thus, it is clear that the different polarization patterns are due to the different excitation wavelengths and not changes in other experimental conditions. It should be noted that the rise time of the triplet spectrum with  $\lambda_{\text{ex}} = 540$  nm is rather slow (ca. 2–3  $\mu\text{s}$ ), whereas that at  $\lambda_{\text{ex}} = 640$  nm (Figure 2) is the same as the response time of the spectrometer ( $\sim 0.5$   $\mu\text{s}$ ).

The spectra obtained with  $\lambda_{\text{ex}} = 540$  nm at 80 K are essentially the same as those reported previously using  $\lambda_{\text{ex}} = 532$  nm and  $T = 77$  K.<sup>16</sup> However, in the present study, the S/N ratio for the TREPR spectra is considerably improved mainly due to the use of the dielectric resonator (see the Experimental Section). In addition, a broad, weak e/a feature is clearly observed over the magnetic field region of ca. 270–420 mT. This signal decays with approximately the same time constant as that of the narrow feature in the center. The latter was tentatively assigned to a quartet or doublet species in which the excited triplet state of the free base and the ground state of the copper porphyrin interact strongly in a closer conformation.<sup>16,20</sup> The narrow emissive feature rises with the response time of the apparatus ( $\tau \approx 0.5$   $\mu\text{s}$ ), and decays more rapidly than the triplet component.

**3.2. Orientation Dependence.** To understand the origin of the differences in the polarization pattern with different excitation wavelengths and to confirm the sign of the spin polarization observed in the isotropic glass, the orientation dependence was studied using a liquid crystal (LC), E7. The ordering in the LC is governed by short-range interactions, and the most probable orientation of the porphyrin plane is coplanar with the LC director.<sup>34–36</sup> By turning the director, L, with respect to the magnetic field, different relative orientations of the porphyrin plane and the field can be achieved. Thus, with the director parallel to the field, the X and Y canonical orientations are most probable and the corresponding spectral features are stronger. Similarly, with the director perpendicular to the field, the features associated with the Z orientation dominate the spectrum.<sup>37</sup> This orientation selection enables us to determine the sign of the polarization for the individual canonical orientations and to confirm the results obtained for the toluene frozen solution.

TREPR spectra of the dimer in E7 are presented in Figure 4 with  $\lambda_{\text{ex}} = 640$  nm (top) and 540 nm (bottom) at 80 K. The solid and dotted lines are the spectra taken with L parallel and perpendicular to the magnetic field, *B*, i.e.,  $B \parallel L$  and  $B \perp L$ , respectively. With  $\lambda_{\text{ex}} = 640$  nm, the polarization pattern of the Z and X orientations is e/a while that of Y is a/e, which is the same as reported for a monomer free base tetraphenyl-

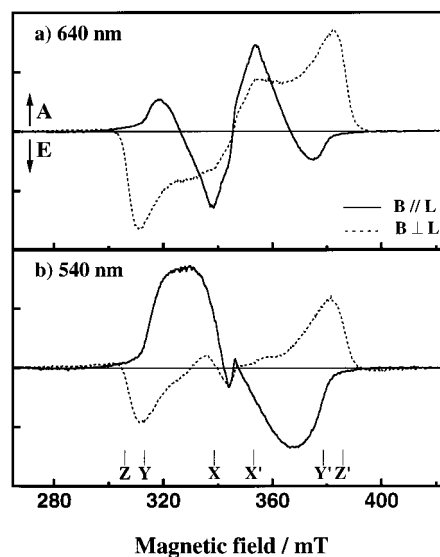


**Figure 4.** Orientation dependence of TREPR spectra of Cu-C<sub>3</sub>-H<sub>2</sub> in E7 at 80 K. The solid lines (—) are the spectra for  $B \parallel L$ , while the dotted lines (---) are for  $B \perp L$ : (a)  $\lambda_{\text{ex}} = 640$  nm, detection gate 1.0–1.5  $\mu\text{s}$  following the laser pulse; (b)  $\lambda_{\text{ex}} = 540$  nm, detection gate 3.0–3.5  $\mu\text{s}$  following the laser pulse.

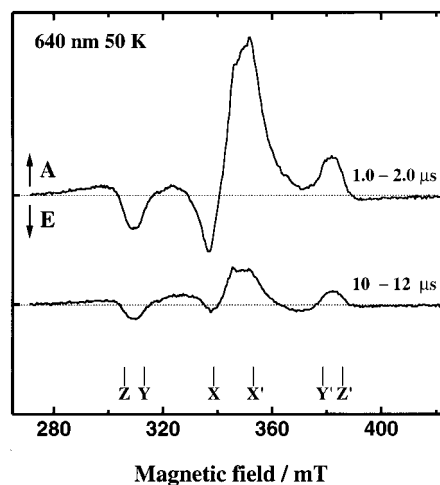


**Figure 5.** TREPR spectra of Cu-C<sub>3</sub>-H<sub>2</sub> in toluene taken with 640 nm excitation at 50 K at early and late times. Top: detection gate 1–2  $\mu\text{s}$  after the laser pulse. Bottom: detection gate 10–12  $\mu\text{s}$ . Other details are the same as for Figure 2.

porphin.<sup>35–37</sup> On the other hand, with selective excitation of the copper(II) half ( $\lambda_{\text{ex}} = 540$  nm), the sign of the polarization associated with the X-canonical orientation is inverted to a/e, while the polarization from the other orientations, i.e., Y and Z, remains a/e and e/a, respectively. Accordingly, the population of the spin states in the two cases is the same for the Y and Z directions, but for the X direction it changes, as consistent with those observed in toluene.

**3.3. Temperature Dependence.** In Figures 5 and 6, spectra taken at  $T = 50$  K are shown which correspond to those in Figures 2 and 3 taken at 80 K. The spectrum obtained for selective excitation at the free base ( $\lambda_{\text{ex}} = 640$  nm) is shown in Figure 5. A careful inspection of Figure 5 reveals that there is a component which has the same ZFS parameters as those of the triplet component at 80 K (Figure 2). However, superimposed on this spectrum, there is an absorptive contribution primarily in the center of the spectral region. The overlap of this component leads to a decrease in the intensity of the emissive maximum and an increase of the absorptive maximum

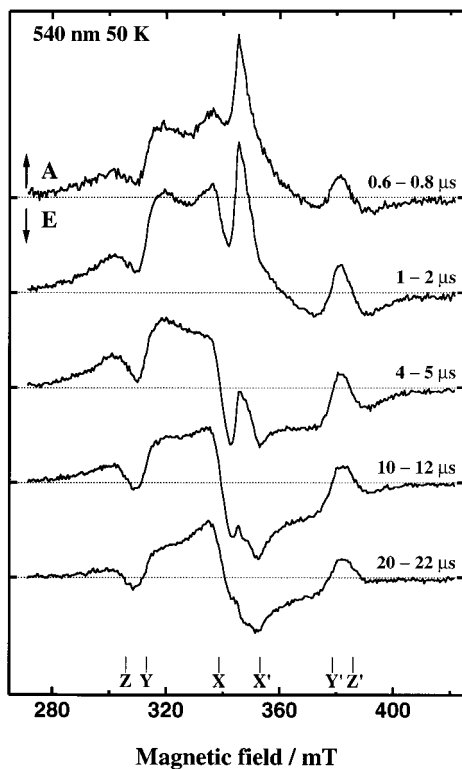


**Figure 6.** Time development of TREPR spectra of Cu-C<sub>3</sub>-H<sub>2</sub> in toluene taken with 540 nm excitation at 50 K. The gate times from top to bottom are 0.6–0.8, 1–2, 4–5, 10–12, and 20–22  $\mu$ s, respectively. Other details are the same as for Figure 2.

compared to the corresponding spectrum at 80 K. The sign of the spin polarization of the triplet component is the same as observed at 80 K (Figure 2). This suggests that the population selectivity for ISC is essentially the same between 80 and 50 K. In analogy to what is seen at 80 K, the signal at the X canonical orientations decays faster.

For  $\lambda_{\text{ex}} = 540$  nm, the two main features found at 80 K (Figure 3) are also observed at 50 K (Figure 6): (i) a triplet-like component which exhibits an eaa/eea polarization pattern (represented by the bottom spectrum taken at a delay time of 20–22  $\mu$ s); (ii) a narrow, emissive feature at the center of the magnetic field accompanied by two broad wings (270–300 and 390–420 mT). However, similar to what is observed with  $\lambda_{\text{ex}} = 640$  nm at 50 K, a new, intense absorptive feature appears around the center of the triplet component spectrum at early delay times. The maximum of this feature is located upfield ( $g = 2.00$ ) from the narrow emissive feature ( $g = 2.02$ ). The rise of this new band is faster than the other components and it decays more rapidly.

#### 4. Discussion

**4.1. Assignment of the “Triplet” Component Spectra.** The “triplet” component observed with  $\lambda_{\text{ex}} = 532$  nm was assigned in ref 16 to the  $T_1$  state of the free base half of the dimer. This assignment is confirmed by the fact that excitation at 640 nm yields a “triplet” spectrum through spin–orbit coupling (SO)–ISC. The observed spin-polarized spectrum is reproduced well using parameters typical of the triplet state of the free base monomer, as shown in Figure 2 (see figure caption for the ZFS parameters). The only significant difference in the parameters for the dimer and the monomer is that the line width is larger in the dimer (2.0 mT for the dimer vs 1.0 mT for the monomer). This is probably due to the spin–spin coupling between the free base triplet and the copper doublet.

For individual orientations of the molecule, the coupling leads to a splitting of the spectral lines. However, if the splitting is of the same magnitude or less than the inhomogeneous line width, it only results in a broadening of the spectrum. The dipolar coupling can be estimated as  $|D| \geq 0.68$  mT from the center-to-center distance of 1.6 nm between the two porphyrins in a possible conformation in which the two moieties are separated at the maximum distance. The exchange coupling is more difficult to estimate. However, values of 0.05–0.1 mT for  $|J|$  have been reported in donor–acceptor systems in which the two spins are separated by 1.6–1.8 nm.<sup>34,38</sup> Consequently, the total spin–spin coupling should be of the order of at least 0.7 mT. On the other hand, if the coupling is larger than this lower limit, significant deviations from a pure triplet spectrum should be observed. On the basis of the above arguments, it is concluded that the spectra of the “triplet” component arise from extended conformations of the molecule in which the coupling is close to the lower limit.

**4.2. Possible Pathways Yielding the “Triplet” Component with an eaa/eea Polarization Pattern.** Before discussing the mechanism which leads to the observed polarization patterns, we need to consider possible pathways which lead to the “triplet” component. The different polarization patterns observed with selective excitation of the two halves of the dimer (see Figures 2–4) can be ascribed to differences in the pathways by which the free base triplet state is generated, since the ZFS parameters are the same. This is also supported by the different rise times with the two excitation wavelengths. (at 80 K,  $\tau \approx 0.5$   $\mu$ s for  $\lambda_{\text{ex}} = 640$  nm vs ca. 2–3  $\mu$ s for  $\lambda_{\text{ex}} = 540$  nm).

Direct excitation of the free base leads to the “triplet” spectrum via SO–ISC. The fact that excitation of the copper-(II) half yields the triplet spectrum, which is different from the SO–ISC spectrum, also suggests that no energy transfer from the  $^2S_1$  of the copper moiety to the  $S_1$  of the free base takes place. This is consistent with the conclusion derived from the fluorescence excitation spectrum of the free base half,<sup>12,16</sup> which is coincident with the absorption spectrum of the free base monomer but not with that of the copper-free base dimer.

The most likely pathway by which excitation of the copper-(II) half could populate the free base triplet is energy transfer via the  $^4T_1$  state of the copper porphyrin as shown in Scheme 1. Although the transient absorption measurements did not suggest any trace of radicals and other intermediates,<sup>12</sup> we cannot completely exclude the possibility that the TREPR and optical experiments could be reporting on different subpopulations generated by different pathways. Thus, we also need to consider the possibility that electron transfer is involved.

**Intramolecular Electron Transfer.** As discussed previously,<sup>16</sup> the polarization pattern observed with selective excitation of the copper moiety (Figures 3, 4, and 6), i.e., the eaa/eea pattern, is consistent with excess population of the spin states with  $T_{+1}$  and  $T_{-1}$  character (see simulation at the bottom of Figure 3). It is conceivable that such a population distribution could be generated by the following electron transfer:<sup>39</sup>



This is analogous to the generation of the triplet states via charge recombination in photosynthetic reaction centers and model compounds.<sup>40–47</sup> In these systems, a radical pair is generated from the excited singlet state of the donor and subsequent S–T<sub>0</sub> mixing in the radical pair leads to recombination to the T<sub>0</sub> state of the donor or acceptor.<sup>40, 48</sup>

In the case of the porphyrin dimer, the radical pair in eq 1 is a three-spin system and the precursor is in a doublet or quartet

state. While the spin dynamics of such a system are quite complicated<sup>49</sup> and depend on the nature of the precursor state, the recombination can be expected to be spin selective. Thus, it is important to examine whether such a reaction is feasible or not.

Generally, whether electron transfer (ET) takes place or not can be discussed in terms of the free energy change before and after the reaction by using the Rehm–Weller equation.<sup>50</sup>

$$\Delta G = -E_{\text{red}}(\text{A}) + E_{\text{ox}}(\text{D}) - E^* - \frac{e^2}{\epsilon a} \quad (2)$$

where  $E_{\text{red}}$  and  $E_{\text{ox}}$  are the reduction potential of the electron acceptor and the oxidation potential of the electron donor, respectively, and  $E^*$  is the energy of the excited state which is the precursor of ET. The last term is the so-called work term in the case of charge separation from the neutral state, with a donor–acceptor distance,  $a$ , and the dielectric constant,  $\epsilon$ , of the solvent.

The Rehm–Weller equation is valid for most polar solvents, but it is not applicable for solvents with low polarity such as toluene because the solvation energy is difficult to estimate. However, experimental and theoretical estimates suggest that  $\Delta G$  in such low polarity solvents is approximately 0.5–0.6 eV higher than predicted by eq 2 and also higher than in polar solvents.<sup>51–53</sup> Therefore, we only need to estimate  $\Delta G$  for the liquid crystal E7 which is more polar than toluene.

The free energy changes in E7 are estimated as  $\Delta G = -0.17$ ,  $+0.23$ , and  $+0.32$  eV for the reactions from the  $^2\text{S}_1$ ,  $^2\text{T}_1$ , and  $^4\text{T}_1$  states in eq 1, respectively.<sup>54</sup> While the large positive values for the  $^2\text{T}_1$  and  $^4\text{T}_1$  states predict that ET is not feasible from these two states, the negative value for the  $^2\text{S}_1$  state suggests that ET is energetically favorable in this case. However, ET from the  $^2\text{S}_1$  state is also very unlikely because it must compete with the fast ( $\tau < 8$  ps) ISC in the copper porphyrin.<sup>31,32</sup> Since the TREPR measurements were carried out in the frozen, glass regime, picosecond ET rates are not expected due to the slow rotational diffusion of the solvent molecules. This is in line with the fact that the ET rates for many donor–acceptor complex systems are attenuated from the picosecond to the microsecond time range in the nematic phase of LCs.<sup>55–57</sup> As a consequence, the electron-transfer pathway can be excluded on energetic grounds from the  $^2\text{T}_1$  and  $^4\text{T}_1$  states and for kinetic reasons from the  $^2\text{S}_1$  state of the copper porphyrin.

**Intramolecular Energy Transfer.** A more plausible explanation for the eaa/eea polarization pattern following the copper half excitation is intramolecular energy transfer via the  $^2\text{T}_1$  or  $^4\text{T}_1$  state of the copper to the free base triplet, as described above. One important question for such a mechanism is whether the lifetime of the precursor state is compatible with the energy transfer rate. In the monomer copper porphyrin, ISC from the  $^2\text{S}_1$  state to the  $^2\text{T}_1$  state takes place on a time scale on the order of picoseconds and proceeds further via relaxation to the  $^4\text{T}_1$  state.<sup>31,32</sup> The relaxation rate from  $^2\text{T}_1$  to  $^4\text{T}_1$  is reported as several hundred picoseconds in a protoporphyrin complex,<sup>31</sup> while in some other copper porphyrins faster rates have been suggested due to the lack of a change in T–T absorption spectra in this time region. In any case, phosphorescence from copper porphyrins at room temperature is assigned to the emission of the  $^2\text{T}_1$  state thermally activated from the  $^4\text{T}_1$  state. At around 80 K, most molecules reside in the  $^4\text{T}_1$  state since the energy gap between the  $^2\text{T}_1$  and  $^4\text{T}_1$  states is much larger than  $kT$ .<sup>26–28</sup> While the observed emission at this temperature is also ascribed to the radiative decay from the  $^2\text{T}_1$  state, the decay rate represents the lifetimes of the  $^4\text{T}_1$  state. In the case of tetraphenyl

and tetratolyl porphyrins, the emission in a glassy medium decays multiexponentially and the spectral shape changes with time ( $< 1 \mu\text{s}$ ).<sup>26,28</sup> Although the emission behavior of these copper porphyrins is somewhat complicated, the slowest component of the kinetic phase has a decay constant of longer than 1 ms at 77 K.<sup>26,28,58</sup> Consequently, the  $^4\text{T}_1$  state, which is primarily populated via the fast relaxation after photoexcitation, is sufficiently long-lived for energy transfer to occur.

On the basis of the above arguments, the observed TREPR spectra with  $\lambda_{\text{ex}} = 540$  nm can be ascribed to triplet excitation of the free base generated via intramolecular energy transfer from the  $^2\text{T}_1$  and/or  $^4\text{T}_1$  excited states of the copper half of the dimer. We will now consider the origin of the observed polarization pattern.

**4.3. Mechanism Leading to the eaa/eea Pattern of the TREPR Spectra.** The polarization pattern of the “triplet” component, observed with  $\lambda_{\text{ex}} = 540$  nm (overpopulation of the states with  $\text{T}_{+1}$  and  $\text{T}_{-1}$  character), is determined by the spin dynamics during the energy transfer process and relaxation in the final metastable state in which the free base is a triplet. Here, we first examine the nature of the spin states before and after the energy transfer and then consider the origin of the polarization pattern specifically.

**Spin States of the Excited States of the Copper(II)–Free Base Porphyrin Dimer.** Following photoexcitation at 540 nm and ISC within the copper moiety, the spin eigenstates of the system are the trip–doublet ( $^2\text{T}_1$ ) and trip–quartet ( $^4\text{T}_1$ ) states of the copper porphyrin. Energy transfer then excites the free base half of the dimer into the triplet state, which is weakly coupled to the copper doublet ground state. In this case, it is instructive to describe the spin eigenstates of the system as linear combinations of either the product states of the triplet (free base) and doublet (copper) components (i.e., the weak coupling limit functions) or the quartet and doublet states (i.e., the strong coupling limit functions) (see Appendix). As discussed above, the coupling between the triplet spins and the copper doublet is fairly weak in the present case (the upper limit of the spin–spin coupling is 1.0 mT; see section 4.1). Under these conditions, the mixing of the product states will be weak and the quartet and doublet character of the eigenstates will be approximately that of the product states:

$$\begin{aligned} \phi_1 &\approx |\text{T}_{+1}, \alpha\rangle = |\text{Q}_{3/2}\rangle \\ \phi_2 &\approx |\text{T}_{+1}, \beta\rangle = \sqrt{\frac{1}{3}}|\text{Q}_{1/2}\rangle + \sqrt{\frac{2}{3}}|\text{D}_{1/2}\rangle \\ \phi_3 &\approx |\text{T}_0, \alpha\rangle = \sqrt{\frac{2}{3}}|\text{Q}_{1/2}\rangle - \sqrt{\frac{1}{3}}|\text{D}_{1/2}\rangle \\ \phi_4 &\approx |\text{T}_0, \beta\rangle = \sqrt{\frac{2}{3}}|\text{Q}_{-1/2}\rangle + \sqrt{\frac{1}{3}}|\text{D}_{-1/2}\rangle \\ \phi_5 &\approx |\text{T}_{-1}, \alpha\rangle = \sqrt{\frac{1}{3}}|\text{Q}_{-1/2}\rangle - \sqrt{\frac{2}{3}}|\text{D}_{-1/2}\rangle \\ \phi_6 &\approx |\text{T}_{-1}, \beta\rangle = |\text{Q}_{-3/2}\rangle \end{aligned} \quad (3)$$

The spin states of the energy donor and acceptor are illustrated graphically in Figure 7. In part A of the figure, the  $^2\text{T}_1$  and  $^4\text{T}_1$  states of the copper half of the dimer are shown, whereas the corresponding eigenstates of the free base triplet–copper doublet ground state are shown in part B. Note that the actual energy separation in part A is larger than that in part B of the figure and that the separation between the  $^2\text{T}_1$  and  $^4\text{T}_1$  states is much larger than indicated. Since the ZFS in copper porphyrins ( $|\text{D}|$

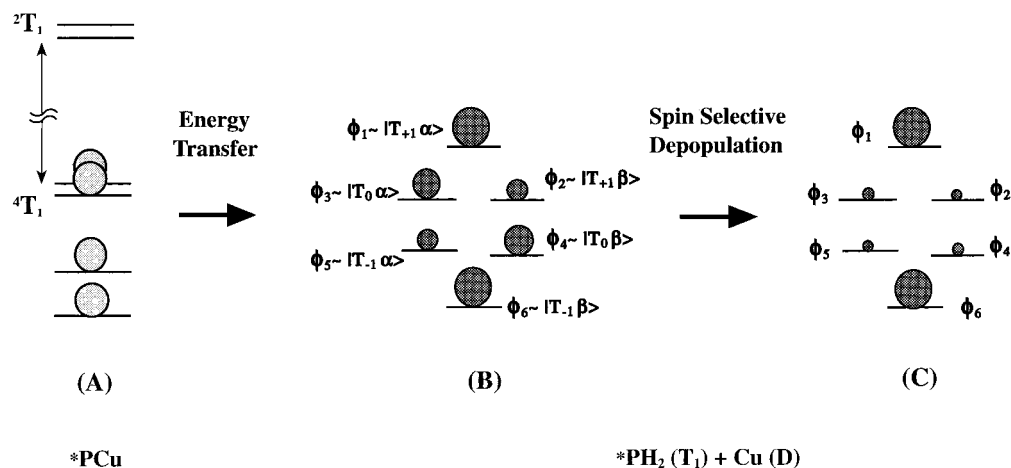


**Figure 7.** Schematic illustration of the spin states involved in the energy transfer from the copper porphyrin (PCu) to the free base (PH<sub>2</sub>) in Cu–C<sub>3</sub>–H<sub>2</sub> (see Scheme 1). The populations of the spin states are indicated by the shaded circles. (A) The trip–quartet (<sup>4</sup>T<sub>1</sub>) and trip–doublet (<sup>2</sup>T<sub>1</sub>) states of PCu. (B) The spin states of the free base triplet weakly coupled to the copper doublet. Population according to the quartet character of the acceptor spin states. (C) Selective depopulation of the spin states according to the doublet character after energy transfer in the weakly coupled triplet–doublet system.

$\approx 0.35 \text{ cm}^{-1}$  and  $|E| = \sim 0.27 \text{ cm}^{-1}$ ,<sup>25,27</sup>) is not small compared to the Zeeman energy at  $B_0 = 300 \text{ mT}$  ( $\sim 0.3 \text{ cm}^{-1}$ ), the quartet state (<sup>4</sup>T<sub>1</sub>, Figure 7A) is close to the zero-field limit and is split into two pairs of spin sublevels. In comparison, the ZFS in part B of Figure 7 is relatively small and the wave functions are almost in the high field limit at  $B_0 = 300 \text{ mT}$ . The energy transfer effectively projects the six states on part A of Figure 7 onto the six states on part B.

*Possible Origins for the eaa/eea Polarization Pattern.* The observed spin polarization pattern with  $\lambda_{\text{ex}} = 540 \text{ nm}$  is attributable to excess population of the spin states with T<sub>+1</sub> and T<sub>-1</sub> character (e.g.,  $\phi_1$  and  $\phi_6$ ). Here, we consider two possible origins for such a population distribution.

(i) The energy transfer from the copper porphyrin could be spin selective such that these states are preferentially populated.

(ii) The polarization could develop through spin-selective electronic relaxation to the ground state.

In general, both the energy transfer and the electronic relaxation can be expected to be spin selective. Thus, possibilities (i) and (ii) are the two limiting cases in which one mechanism dominates. If possibility (i) holds, the rise time of the triplet component ( $2\text{--}3 \mu\text{s}$ ) would correspond to the energy transfer rate. On the other hand, if possibility (ii) holds, then the rise of the signal corresponds to the difference in the lifetimes of the spin states and the selective electronic relaxation must be faster than the spin relaxation.

*Spin-Selective Energy Transfer via the Trip–Quartet State of the Copper(II) Half.* A simple explanation for the overpopulation, i.e., possibility (i), could be that the ISC and spin dynamics within the copper moiety lead to selective population of the  $S_z = \pm 3/2$  sublevels in the <sup>4</sup>T<sub>1</sub> state of the copper. The projection of this population distribution onto the spin states in the free base triplet–copper(II) doublet system (part B of Figure 7) would then populate only states  $\phi_1$  and  $\phi_6$  because they correspond to the states  $|Q_{3/2}\rangle$  and  $|Q_{-3/2}\rangle$ , respectively. However, we can exclude this possibility because the spin states in the copper <sup>4</sup>T<sub>1</sub> state are not in the high-field limit and  $S_z$  is not a good quantum number. Moreover, it is likely that rapid spin relaxation takes place in the <sup>4</sup>T<sub>1</sub> state leading to rapid equilibration among the sublevels.

If we assume fast spin relaxation in the <sup>4</sup>T<sub>1</sub> state, the subsequent energy transfer will populate the spin states of the weakly coupled triplet–doublet pair solely according to their

quartet character. This assumption that spin relaxation takes place rapidly in the copper <sup>4</sup>T<sub>1</sub> state is very reasonable because no spin polarization is observed at 20–300 K with X-band microwave and because a large  $|D|$  value, reported from experiments at very low temperatures ( $\leq 4.2 \text{ K}$ ),<sup>25,27</sup> is expected to cause rapid relaxation. The resultant population distribution due to the energy transfer is indicated by the shaded circles in part B of Figure 7. The EPR spectrum from this population distribution consists of pairs of oppositely polarized transitions. For example, the two transitions  $\phi_1 \leftarrow \phi_3$  and  $\phi_2 \leftarrow \phi_4$  correspond approximately to the  $|T_{+1}\rangle \leftarrow |T_0\rangle$  transition in the free base triplet for the two orientations  $\alpha, \beta$  of the doublet spin. The population differences for these two transitions are

$$I_{13} \propto -\Delta P_{13} = -\frac{1}{3} \quad (4)$$

$$I_{24} \propto -\Delta P_{24} = +\frac{1}{3} \quad (5)$$

Obviously, their intensities are equal and opposite. Similarly, the total intensity of the pair of transitions  $\phi_3 \leftarrow \phi_5$  and  $\phi_4 \leftarrow \phi_6$ , which correspond to the  $|T_0\rangle \leftarrow |T_{-1}\rangle$  transition, is also zero. In the extreme case of no coupling between the doublet and triplet, the pairs of transitions are degenerate and their intensities cancel each other completely. However, as discussed above, the coupling in the dimer is expected to be roughly as large as the inhomogeneous line width. Therefore, the spectral contributions from the pairs of transitions will overlap to a large extent but will not cancel each other completely. The resulting polarization pattern summed over all orientations (not shown) resembles the first derivative of the triplet spectrum in thermal equilibrium and is roughly a factor of 10–20 weaker than the simulation shown in Figure 3. Although the possibility that such a spectrum makes a weak contribution to the experimental data cannot be ruled out, it does not account for the eaa/eea pattern observed with  $\lambda_{\text{ex}} = 540 \text{ nm}$ .

*Spin-Selective Electronic Relaxation Following Energy Transfer via the Trip–Quartet State.* The second possibility is that selective depopulation of the spin states occurs. It is likely that the states with doublet character relax more rapidly because the ground state is a doublet. This process corresponds to parts B and C of Figure 7. We can assign two rate constants,  $k_Q$  and  $k_D$ , to the electronic relaxation from a pure quartet and a pure

doublet state, respectively. The relaxation from  $\phi_1 \cdots \phi_6$ , will then be governed by rate constants which are linear combinations of  $k_Q$  and  $k_D$ . In general, these rate constants will be different and the polarization pattern will change with time.

Assuming that (i) the electronic relaxation from the quartet states is slow, i.e.,  $k_Q \approx 0$ , and (ii) the spin relaxation rate is slow compared with the depopulation rate,  $k_D$ , the following time-dependent intensities are obtained as the products of the transition probability and population differences.

“Triplet” transitions:

$$|T_{+1}\rangle \leftarrow |T_0\rangle$$

$$I_{13}(t) \propto -\left\{1 - \frac{2}{3} \exp\left(\frac{-k_D t}{3}\right)\right\} \quad (6)$$

$$I_{24}(t) \propto -\left\{\frac{1}{3} \exp\left(\frac{-2k_D t}{3}\right) - \frac{2}{3} \exp\left(\frac{-k_D t}{3}\right)\right\} \quad (7)$$

$$|T_0\rangle \leftarrow |T_{-1}\rangle$$

$$I_{35}(t) \propto \left\{\frac{1}{3} \exp\left(\frac{-2k_D t}{3}\right) - \frac{2}{3} \exp\left(\frac{-k_D t}{3}\right)\right\} \quad (8)$$

$$I_{46}(t) \propto \left\{1 - \frac{2}{3} \exp\left(\frac{-k_D t}{3}\right)\right\} \quad (9)$$

Because the energy transfer via the  ${}^4T_1$  state populates the spin states according to their quartet character under the assumption of rapid spin relaxation in the energy donor, the intensities at  $t = 0$  are the same as those in the discussion for possibility (i). Therefore, the intensity at early times will be weak. However, as the states are depopulated, the intensities of the transitions will become unequal and at long times only transitions  $I_{13}$  and  $I_{46}$  which correspond to the triplet transitions  $|T_{+1}\rangle \leftarrow |T_0\rangle$  and  $|T_0\rangle \leftarrow |T_{-1}\rangle$  will have appreciable intensity. This is a result of the fact that the two states  $\phi_1$  and  $\phi_6$ , are pure quartet states and also have only  $T_{+1}$  and  $T_{-1}$  character. Thus, these states will be longer lived and the spin-selective relaxation to the ground-state results in a spectrum which corresponds to the  $T_{+1}$  and  $T_{-1}$  overpopulation.

In the above mechanism, the energy transfer rate should be  $k_{EIT} \gg (1\mu s)^{-1}$  and the rise time of the triplet spectrum will correspond roughly to the relaxation rate,  $k_D$ . Since the depopulation takes place after the formation of the free base triplet, the effect should also contribute to the time development of the spectra with the selective excitation of the free base half. This is indeed observed in the signal decays with  $\lambda_{ex} = 640$  nm and their orientation dependence (Figures 2 and 5). At the  $X$ -canonical orientation, the major component of the signal decay is  $\sim 2\mu s$ , which is much faster than the corresponding decay in the monomer and almost coincident with the rise time of the eaa/eea component observed with  $\lambda_{ex} = 540$  nm.<sup>59</sup> This observation supports the presented mechanism, i.e., the spin-selective electronic depopulation from the excited state.

In contrast to the  $X$ -canonical orientation, the signal decays corresponding to the  $Z$ -orientations, with excitation of the free base half ( $\lambda_{ex} = 640$  nm), are only slightly faster than those of the free base monomer and are different from the rise time for  $\lambda_{ex} = 540$  nm. This orientation dependence also supports the selective depopulation, which is subjected to orientation dependence of the initial population in the case of ISC. The effect of the depopulation on the signal decays is expected for the orientations in which ISC yields dominant population into  $\phi_2$ ,  $\phi_3$ ,  $\phi_4$ , and  $\phi_5$  states but not expected when ISC populates  $\phi_1$  and  $\phi_6$  states. This is because the selective electronic relaxation

can take place only from  $\phi_2$ ,  $\phi_3$ ,  $\phi_4$ , and  $\phi_5$  states (see Figure 7C). In the free base, ISC predominantly populates states with  $x$ -symmetry. This means that spin states with  $T_0$  character ( $\phi_3$  and  $\phi_4$ ) are populated with  $B \parallel X$ , whereas with  $B \parallel Z$ , states with  $T_{+1}$  and  $T_{-1}$  character ( $\phi_1$ ,  $\phi_2$ ,  $\phi_5$  and  $\phi_6$ ) are populated almost equally. Thus, the selective relaxation should affect the signal decay for the  $X$ -canonical orientation strongly but should only have a weak influence for the  $Z$ -orientation, as observed.

*Spin Polarization Patterns Expected by Energy Transfer via the Trip–Doublet State of the Copper Porphyrin Half.* As shown above, the selective depopulation following the energy transfer via the  ${}^4T_1$  state of the copper(II) porphyrin half explains not only the eaa/eea polarization pattern with  $\lambda_{ex} = 540$  nm but also the orientation dependence of the signal decays with  $\lambda_{ex} = 640$  nm. In the previous two subsections, we have assumed energy transfer takes place via the  ${}^4T_1$  state of the copper(II), since most molecules relax into the  ${}^4T_1$  state immediately after the excitation of the copper half as discussed in section 4.2. However, energy transfer might take place from the trip–doublet state which could be thermally activated from the  ${}^4T_1$  state. In a manner similar to the above, we can examine the expected spin polarization pattern caused by energy transfer through the  ${}^2T_1$  state of the copper(II).

For energy transfer from the thermally populated  ${}^2T_1$  state, the following time dependence of the EPR transitions are obtained by assuming (i) population of the free base triplet–copper doublet spin states according to their doublet character and (ii) spin-selective depopulation from the spin states also according to their doublet character (only transitions corresponding to  $|T_{+1}\rangle \leftarrow |T_0\rangle$  are shown below).

“Triplet” ( $|T_{+1}\rangle \leftarrow |T_0\rangle$ ) transitions:

$$I_{13}(t) \propto \left\{\frac{1}{3} \exp\left(\frac{-k_D t}{3}\right)\right\} \quad (10)$$

$$I_{24}(t) \propto \left\{-\frac{2}{3} \exp\left(\frac{-2k_D t}{3}\right) + \frac{1}{3} \exp\left(\frac{-k_D t}{3}\right)\right\} \quad (11)$$

Similar to the energy transfer directly from the  ${}^4T_1$  state, the total intensity for the pair of transitions at  $t = 0$  is zero, and the population from the  ${}^2T_1$  state also will yield a very weak spectrum which resembles the first derivative of the triplet spectrum (with the opposite phase to that from the  ${}^4T_1$  state). As time increases, the selective depopulation due to the doublet character induces unequal intensities for the pairs of transitions. However, in contrast to the direct energy transfer from the  ${}^4T_1$  state, the total intensity for  $|T_{+1}\rangle \leftarrow |T_0\rangle$  is positive whereas that for  $|T_0\rangle \leftarrow |T_{-1}\rangle$ , i.e.,  $I_{35} (= -I_{24})$  and  $I_{46} (= -I_{13})$ , is negative. These lead to a triplet-like spectrum corresponding to excess  $T_0$  population. Although further depopulation leads to no intensity for the spectrum at longer delay times, during the depopulation, the spin-polarized spectrum appears with an aee/aae pattern which is reversed to that observed in the dimer. As a consequence, the energy transfer via the  ${}^2T_1$  state as well as that followed by the spin-selective depopulation is inconsistent with the observed results and cannot be the origin for the eaa/eea polarization pattern.

*Doublet Signals.* In the above discussion, we have ignored the transitions  $\phi_2 \leftarrow \phi_1$ ,  $\phi_4 \leftarrow \phi_3$ , and  $\phi_6 \leftarrow \phi_5$  which correspond to a flip of doublet spin, i.e.,  $|\alpha\rangle \leftarrow |\beta\rangle$ . The population difference for transition  $\phi_4 \leftarrow \phi_3$  is zero, and the separation of transitions  $\phi_2 \leftarrow \phi_1$  and  $\phi_6 \leftarrow \phi_5$  is twice as large as the doublet–triplet splitting. Assuming energy transfer directly from the  ${}^4T_1$  state of the copper(II), the spin-selective relaxation leads to the following time dependence.

“Doublet” transitions,  $|\alpha\rangle \leftarrow |\beta\rangle$ :

$$I_{12}(t), I_{56}(t) \propto \pm \left\{ \frac{1}{3} \exp\left(\frac{-2k_D t}{3}\right) - 1 \right\} \quad (12)$$

$$I_{34}(t) \approx 0 \quad (13)$$

Because  $I_{12}$  and  $I_{56}$  have the same time dependence, the contribution from these transitions will be weak due to the cancellation effects discussed for possibility (i). Although eq 10 suggests that the spectral contribution from the copper doublet will increase with time due to an increasing of individual intensities, it will also remain weak for the same reason. In agreement with this prediction, we do not observe spin-polarized spectra of the copper doublet.

Although the spin-selective depopulation of the weakly coupled triplet–doublet system is formally analogous to the spin selective recombination of a radical pair in the presence of an observer spin,<sup>49</sup> there is a significant difference in spin polarization in the doublet spins. In contrast to such a recombination process which will generally lead to appreciable polarization in the observer doublet, it is noted that our weakly coupled dimer results in apparently very weak spin polarization of the copper doublet following relaxation of the triplet. Calculations aimed at investigating the relationships between the magnetic properties of the system and the polarization of the doublet state are currently in progress.

On the basis of the evidence presented above, we conclude that the observed polarization of the “triplet” component with  $\lambda_{\text{ex}} = 540$  nm is a result of intramolecular energy transfer directly from the  $^4T_1$  state and subsequent selective depopulation of the states according to their doublet character.

#### 4.4. Narrow Emission and Absorption Bands Observed in the Center of the Spectral Region and Broad Wings.

*Narrow Emission and Absorption Bands.* As seen in Figures 3 and 6, a narrow emission band is observed at around the center of the triplet component spectra at both 50 and 80 K with  $\lambda_{\text{ex}} = 540$  nm. In addition, an absorption band appears approximately 2 mT upfield from the emissive feature when the temperature is decreased to 50 K. Because the bridging group between the two porphyrins is a flexible three-carbon chain, several conformations of the dimer are possible.<sup>16,20</sup> It is likely that these two bands are due to a species in which the coupling between the free base triplet and copper doublet is strong. In this case, the spin states split into doublet and quartet states (see Appendix).<sup>60–64</sup>

Under the condition that the  $J$ -coupling is much larger than the Zeeman energies and dipole–dipole coupling,  $g$ -factors for the quartet and doublet states generated in the coupled triplet (A)–doublet (B) system are given by<sup>64</sup>

$$g_Q = \frac{2}{3}g_A + \frac{1}{3}g_B \quad (14)$$

$$g_D = \frac{4}{3}g_A - \frac{1}{3}g_B \quad (15)$$

Assuming that  $g_A = 2.008$  (free base triplet) and  $g_B = 2.055$  (the ground state copper, perpendicular),<sup>65</sup> values of 2.024 and 1.992 are calculated for  $g_Q$  and  $g_D$ , respectively. Thus, the resonance field of the doublet state is expected upfield from that of the quartet. The observed  $g$ -factors are 2.02 and 2.00 for the peak positions of the emission and absorption bands, respectively. These values correspond reasonably well with the estimated  $g$ -factors and suggest that the emission band is the

$m_s = \pm 1/2$  transition of the quartet while the absorption band is a doublet. A faster decay of the absorption band is also consistent with this assignment since the doublet state should have a shorter lifetime.

*Broad Wings of the Spectra.* In addition to the narrow emissive and absorptive bands, there are broad contributions which exhibit absorption in the lower magnetic field ( $\sim 270$ – $300$  mT) and emission in the higher magnetic field ( $\sim 390$ – $420$  mT) (see Figures 3 and 6). These two wings have almost identical decay kinetics to that of the narrow band, which suggests that they belong to the same species and implies that they are the  $m_s = \pm 3/2 \leftrightarrow \pm 1/2$  transitions of the quartet.

In the strong coupling limit, the quartet ZFS is given by

$$D_Q = \frac{1}{3}D_T + \frac{1}{3}D_{TD} \quad (16)$$

<sup>64</sup> where  $D_Q$  and  $D_T$  are the quartet and triplet ZFS parameters, respectively, and  $D_{TD}$  is the coupling between the doublet and triplet. From eq 16, it is expected that  $D_Q < D_T$ , i.e., the quartet spectrum is not broader than the triplet, unless  $D_{TD}$  is more than twice as large as  $D_T$ . Since the observed features are broader than the “triplet” component, this assignment might imply an unreasonably strong dipolar coupling between the triplet and doublet. However, the EPR spectrum of the ground state copper porphyrin extends over ca. 100 mT due to large hyperfine coupling, and thus the observed broad spectra are likely to be a result of the large hyperfine interaction ascribed to the copper(II) doublet. Experiments with higher microwave frequencies and their analysis taking account of the anisotropic  $g$ -values and hyperfine coupling of the ground-state copper(II) are in progress and may lead to a better separation of the contributions and a more complete understanding of both the narrow bands in the center and broad wings of the spectrum.

## 5. Conclusions

Selective excitation of the individual halves of the dimer leads to the conclusion that intramolecular energy transfer takes place directly from the copper(II) trip–quartet state to the free base triplet. However, subsequent spin-selective depopulation in the energy acceptor appears to also play a crucial role in determining the observed polarization pattern. This spin-selective depopulation is rationalized in terms of electronic relaxation to the ground state due to the doublet character of the spin states of the energy acceptor, where the free base triplet is weakly coupled with the ground state copper(II) doublet. Here, it is noteworthy that TREPR measurements using selective excitation of both the energy donor and acceptor provide clear evidence of the dynamics of the molecular electronic states through the consistent rise and decay of the EPR signals resulting from this depopulation.

On the other hand, the decay kinetics and  $g$ -factors of the additional features in the center of the spectrum suggest that they are the doublet and quartet states in conformations of the dimer in which the two halves interact strongly. These results lead to the suggestion that electronic dynamics in molecular systems involving a paramagnetic metal can vary to a large extent through the interaction with the remote spins. We are currently studying a series of similar dimers with rigid bridging groups in which the strength of the coupling strength between the triplet and doublet can be varied systematically.

## Appendix

The spin states in a coupled triplet–doublet system can be described as follows:

$$\phi_1 = |T_{+1}\alpha\rangle = |Q_{3/2}\rangle$$

$$\begin{aligned} \phi_2 &= \cos \theta |T_{+1}\beta\rangle + \sin \theta |T_0\alpha\rangle \\ &= \left( \sqrt{\frac{1}{3}} \cos \theta + \sqrt{\frac{2}{3}} \sin \theta \right) |Q_{1/2}\rangle + \\ &\quad \left( \sqrt{\frac{2}{3}} \cos \theta - \sqrt{\frac{1}{3}} \sin \theta \right) |D_{1/2}\rangle \end{aligned}$$

$$\begin{aligned} \phi_3 &= -\sin \theta |T_0\alpha\rangle + \cos \theta |T_{+1}\beta\rangle \\ &= \left( \sqrt{\frac{2}{3}} \cos \theta - \sqrt{\frac{1}{3}} \sin \theta \right) |Q_{1/2}\rangle - \\ &\quad \left( \sqrt{\frac{1}{3}} \cos \theta + \sqrt{\frac{2}{3}} \sin \theta \right) |D_{1/2}\rangle \end{aligned}$$

$$\begin{aligned} \phi_4 &= \cos \varphi |T_0\beta\rangle + \sin \varphi |T_{-1}\alpha\rangle \\ &= \left( \sqrt{\frac{2}{3}} \cos \varphi + \sqrt{\frac{1}{3}} \sin \varphi \right) |Q_{-1/2}\rangle + \\ &\quad \left( \sqrt{\frac{1}{3}} \cos \varphi - \sqrt{\frac{2}{3}} \sin \varphi \right) |D_{-1/2}\rangle \end{aligned}$$

$$\begin{aligned} \phi_5 &= -\sin \varphi |T_0\beta\rangle + \cos \varphi |T_{-1}\alpha\rangle \\ &= \left( \sqrt{\frac{1}{3}} \cos \varphi - \sqrt{\frac{2}{3}} \sin \varphi \right) |Q_{-1/2}\rangle - \\ &\quad \left( \sqrt{\frac{2}{3}} \cos \varphi + \sqrt{\frac{1}{3}} \sin \varphi \right) |D_{-1/2}\rangle \end{aligned}$$

$$\phi_6 = |T_{-1}\beta\rangle = |Q_{-3/2}\rangle$$

In the weak coupling limit,  $\cos \theta = \cos \varphi = 1$ ,  $\sin \theta = \sin \varphi = 0$  and the eigenstates  $\phi_2 \cdots \phi_5$  become the product states  $|T_{+1}\beta\rangle$ ,  $|T_0\alpha\rangle$ ,  $|T_0\beta\rangle$ , and  $|T_{-1}\alpha\rangle$ , respectively. In the strong coupling limit,  $\cos \theta = \sqrt{2}/3$ ,  $\sin \theta = -\sqrt{1}/3$ ,  $\cos \varphi = \sqrt{2}/3$ ,  $\sin \varphi = \sqrt{1}/3$ , and the eigenstates  $\phi_2 \cdots \phi_5$  are  $|Q_{\pm 1/2}\rangle$  and  $|D_{\pm 1/2}\rangle$ .

**Acknowledgment.** This work was supported by the Deutsche Forschungsgemeinschaft Sfb 337. M.A. thanks the JSPS for a fellowship for research at centers of excellence abroad.

## References and Notes

- (1) (a) Ward, M. R. *Chem. Soc. Rev.* **1997**, 26, 365. (b) Kurreck, H.; Huber, M. *Angew. Chem., Int. Ed. Engl.* **1995**, 34, 849. (c) Wasielewski, M. R. *Chem. Rev.* **1992**, 92, 435. (d) Sessler, J. L. *Isr. J. Chem.* **1992**, 32, 449. (e) Gust, D.; Moore, T. A. *Adv. Photochem.* **1991**, 16, 1.
- (2) (a) Osuka, A.; Maruyama, K. *J. Am. Chem. Soc.* **1988**, 110, 4454. (b) Osuka, A.; Maruyama, K.; Yamazaki, I.; Tamai, N. *J. Chem. Soc., Chem. Commun.* **1988**, 1243.
- (3) (a) Rodriguez, J.; Kirmaier, C.; Johnson, M. R.; Frienner, R. A.; Holten, D.; Sessler, J. L. *J. Am. Chem. Soc.* **1991**, 113, 1652. (b) Sessler, J. L.; Hugdahl, J.; Johnson, M. R. *J. Org. Chem.* **1986**, 51, 2838.
- (4) (a) Hsiao, J.-S.; Krueger, B. P.; Wagner, R. W.; Johnson, T. E.; Delaney, J. K.; Mauzerall, D. C.; Fleming, G. R.; Lindsey, J. S.; Bocian, D. F.; Donohoe, R. J. *J. Am. Chem. Soc.* **1996**, 118, 11181. (b) Strachan, J.-P.; Gentemann, S.; Seth, J.; Kalsbeck, W. A.; Linsey, J. S.; Holten, D.; Bocian, D. F. *J. Am. Chem. Soc.* **1997**, 119, 11191. (c) Strachan, J.-P.; Gentemann, S.; Seth, J.; Kalsbeck, W. A.; Linsey, J. S.; Holten, D.; Bocian, D. F. *Inorg. Chem.* **1998**, 37, 1191.
- (5) Jensen, K. K.; van Berlekom, S. B.; Kajanus, J.; Mårtensson, J.; Albinsson, B. *J. Phys. Chem. A* **1997**, 101, 2218.
- (6) (a) Osuka, A.; Maruyama, K.; Yamazaki, I.; Tamai, N. *Chem. Phys. Lett.* **1990**, 165, 392. (b) Osuka, A.; Tanabe, N.; Kawabata, S.; Yamazaki, I.; Nishimura, Y. *J. Org. Chem.* **1995**, 60, 7177. (c) Kawabata, S.; Yamazaki, I.; Nishimura, Y.; Osuka, A. *J. Chem. Soc., Perkin Trans. 2* **1997**, 101, 479.
- (7) (a) Brookfield, R. L.; Ellul, H.; Harriman, A.; Porter, G. *J. Chem. Soc., Faraday Trans. 2* **1986**, 82, 219. (b) Anton, J. A.; Loach, P. A.; Govindjee, *Photochem. Photobiol.* **1978**, 28, 235.
- (8) (a) Regev, A.; Galili, T.; Levanon, H.; Harriman, A. *Chem. Phys. Lett.* **1986**, 131, 140. (b) Gonen, O.; Levanon, H. *J. Chem. Phys.* **1986**, 84, 4132.
- (9) Sessler, J. L.; Wang, B.; Harriman, A. *J. Am. Chem. Soc.* **1995**, 117, 704.
- (10) (a) Gust, D.; Moore, T. A.; Moore, A. L.; Gao, F.; Luttrull, D.; DeGraziano, J. M.; Ma, X. C.; Makings, L. R.; Lee, S.-J.; Trier, T. T.; Bittersmann, E.; Seely, G. R.; Woodward, S.; Bensasson, R. V.; Rougée, M.; De Schryver, F. C.; Van der Auweraer, M. *J. Am. Chem. Soc.* **1991**, 113, 3638. (b) Gust, D.; Moore, T. A.; Moore, A. L.; Leggett, L.; Lin, S.; DeGraziano, J. M.; Hermant, R. M.; Nicodem, D.; Craig, P.; Seely, G. R.; Nieman, R. A. *J. Phys. Chem.* **1993**, 97, 7926. (c) Gust, D.; Moore, T. A.; Moore, A. L.; Devadoss, C.; Liddell, P. A.; Hermant, R.; Nieman, R. A.; Demanche, L. J.; DeGraziano, J. M.; Gouni, I. *J. Am. Chem. Soc.* **1992**, 114, 3590.
- (11) (a) Mialocq, J. C.; Giannotti, C.; Maillard, P.; Mometeau, M. *Chem. Phys. Lett.* **1984**, 112, 87. (b) Schwarz, F. P.; Gouterman, M.; Muljani, Z.; Dolphin, D. H. *Bioinorg. Chem.* **1972**, 2, 1.
- (12) Ohno, O.; Ogasawara, Y.; Asano, M.; Kajii, Y.; Kaizu, Y.; Obi, K.; Kobayashi, H. *J. Phys. Chem.* **1987**, 91, 4269.
- (13) (a) de Rege, P. J. F.; Williams, S. A.; Therien, M. J. *Since 1995*, 269, 1409. (b) de Rege, P. J. F.; Therien, M. J. *Inorg. Chim. Acta* **1996**, 242, 211.
- (14) Osuka, A.; Maruyama, K.; Mataga, N.; Asahi, T.; Yamazaki, I.; Tamai, N. *J. Am. Chem. Soc.* **1990**, 112, 4958.
- (15) (a) Harriman, A.; Heitz, V.; Ebersole, M.; van Willigen, H. *J. Phys. Chem.* **1994**, 98, 4982. (b) Chambron, J.-C.; Harriman, A.; Heitz, V.; Sauvage, J.-P. *J. Am. Chem. Soc.* **1993**, 115, 6109. (c) Harriman, A.; Odebel, F.; Sauvage, J.-P. *J. Am. Chem. Soc.* **1995**, 117, 9461.
- (16) Asano-Someda, M.; Ichino, T.; Kaizu, Y. *J. Phys. Chem. A* **1997**, 101, 4484.
- (17) Hugerat, M.; van der Est, A.; Ojadi, E.; Biczok, L.; Linschitz, H.; Levanon, H.; Stehlik, D. *J. Phys. Chem.* **1996**, 100, 495.
- (18) Tsuchiya, S. *J. Am. Chem. Soc.* **1999**, 121, 48.
- (19) (a) Hugerat, M.; Levanon, H.; Ojadi, E.; Biczok, L.; Linschitz, H. *Chem. Phys. Lett.* **1991**, 181, 400. (b) Levanon, H.; Regev, A.; Galili, T.; Hugerat, M.; Chang, C.-K.; Fajer, J. *J. Phys. Chem.* **1993**, 97, 13198. (c) Berg, A.; Rachamim, M.; Galili, T.; Levanon, H. *J. Phys. Chem.* **1996**, 100, 8791.
- (20) Kaizu, Y.; Maekawa, H.; Kobayashi, H. *J. Phys. Chem.* **1986**, 90, 4234.
- (21) Förster, T. *Discuss. Faraday Soc.* **1959**, 27, 7.
- (22) Dexter, D. L. *J. Chem. Phys.* **1953**, 21, 836.
- (23) McConnel, H. M. *J. Chem. Phys.* **1961**, 35, 508.
- (24) Ake, R. L.; Gouterman, M. *Theor. Chim. Acta* **1969**, 15, 20.
- (25) (a) van Dorp, W. G.; Canters, G. W.; van der Waals, J. H. *Chem. Phys. Lett.* **1975**, 35, 450. (b) van Dijk, N.; van der Waals, J. H. *Mol. Phys.* **1979**, 38, 1211. (c) Noort, M.; Jansen, G.; Canters, G. W.; van der Waals, J. H. *Spectrochim. Acta* **1976**, 32, 1371.
- (26) (a) Gouterman, M.; Mathies, R. A.; Smith, B. E.; Caughey, W. S. *J. Chem. Phys.* **1970**, 52, 3795. (b) Eastwood, D.; Gouterman, M. *J. Mol. Spectrosc.* **1969**, 30, 437.
- (27) (a) van der Poel, W. A. J. A.; Nuijs, A. M.; van der Waals, J. H. *J. Phys. Chem.* **1986**, 90, 1537. (b) van Dijk, N.; Noort, M.; van der Waals, J. H. *Mol. Phys.* **1979**, 44, 891.
- (28) (a) Asano, M.; Kaizu, Y.; Kobayashi, H. *J. Chem. Phys.* **1988**, 89, 6567. (b) Asano-Someda, M.; Kaizu, Y. *J. Photochem. Photobiol. A* **1995**, 87, 23.
- (29) Yan, X.; Holten, D. *J. Phys. Chem.* **1988**, 92, 5982.
- (30) Cunningham, K. L.; McNett, K. M.; Pierce, R. A.; Davis, K. A.; Harris, H. H.; Flack, D. M.; McMillin, D. R. *Inorg. Chem.* **1997**, 36, 608.
- (31) Kobayashi, T.; Huppert, D.; Straub, K. D.; Renzepis, P. M. *J. Chem. Phys.* **1979**, 70, 1720.
- (32) Rodriguez, J.; Kirmaier, C.; Holten, D. *J. Am. Chem. Soc.* **1989**, 111, 6500.
- (33) Gouterman, M. In *The Porphyrins*; Dolphin, D., Ed.; Academic Press: New York, 1978; Vol. 3, p 1.
- (34) (a) van der Est, A.; Fuechsle, G.; Stehlik, D.; Wasielewski, M. R. *Appl. Magn. Reson.* **1997**, 13, 317. (b) van der Est, A.; Fuechsle, G.; Stehlik, D.; Wasielewski, M. R. *Ber. Bunsen-Ges. Phys.* **1996**, 12, 2081.
- (35) Regev, A.; Galili, T.; Levanon, H. *J. Chem. Phys.* **1990**, 92, 4718.
- (36) (a) Gonen, O.; Levanon, H. *J. Phys. Chem.* **1985**, 89, 1637. (b) Gonen, O.; Levanon, H. *J. Phys. Chem.* **1984**, 88, 4223.
- (37) Levanon, H. *Rev. Chem. Int.* **1987**, 8, 287.
- (38) (a) Berman, A.; Izraeli, E. S.; Levanon, H.; Wang, B.; Sessler, J. L. *J. Am. Chem. Soc.* **1995**, 117, 8252. (b) Asano-Someda, M.; Levanon, H.; Sessler, J. L.; Wang, R. *Mol. Phys.* **1998**, 95, 935.
- (39) The reaction,  $\text{TPPCu} + \text{TPPH}_2 \rightarrow \text{TPPCu}^- + \text{TPPH}_2^+$ , requires larger energy ( $E_{\text{red}} = -1.20$ ,  $E_{\text{ox}} = 0.95$  (eV)) than that of  $\text{TPPCu} + \text{TPPH}_2 \rightarrow \text{TPPCu}^+ + \text{TPPH}_2^-$  ( $E_{\text{red}} = -1.05$ ,  $E_{\text{ox}} = 0.90$  (eV)).

- (40) Thurnauer, M. C.; Katz, J. J.; Norris, J. R. *Proc. Nat. Acad. Sci., U.S.A.* **1975**, *72*, 3270.
- (41) Dutton, P. L.; Leigh, J. S.; Seibert, M. *Biochem. Biophys. Res. Commun.* **1972**, *46*, 406.
- (42) McGann, W. J.; Frank, H. A. *Chem. Phys. Lett.* **1985**, *121*, 253.
- (43) Hoff, A. J. *Phys. Rep.* **1979**, *54*, 75.
- (44) Gast, P.; Wasielewski, M. R.; Schiffer, M.; Norris, J. R. *Nature* **1983**, *305*, 451.
- (45) Hasharoni, K.; Levanon, H.; Greenfield, S. R.; Gosztola, D. J.; Svec, W. A.; Wasielewski, M. R. *J. Am. Chem. Soc.*, **1996**, *118*, 10228.
- (46) Carbonera, D.; Di Valentin, M.; Corvaja, C.; Agostini, G.; Giacometti, G.; Liddel, P. A.; Kuciauskas, D.; Moore, A. L.; Moore, T. A.; Gust, D. *J. Am. Chem. Soc.* **1998**, *120*, 4398.
- (47) (a) Scherz, A.; Levanon, H. *J. Phys. Chem.* **1980**, *84*, 324. (b) Nechushtai, R.; Nelson, N.; Gonen, O. Levanon, H. *Biochim. Biophys. Acta* **1985**, *807*, 35.
- (48) Levanon, H.; Norris, J. R. *Chem. Rev.* **1978**, *78*, 185.
- (49) Salikhov, K.; van der Est, A.; Stehlik, D. *Appl. Magn. Res.*, in press.
- (50) Rehm, D.; Weller, A. *Isr. J. Chem.* **1970**, *8*, 259.
- (51) Weller, A. *Z. Phys. Chem. (Munich)* **1982**, *133*, 93.
- (52) Wasielewski, M. R.; Gaines, G. L., III.; O'Neil, M. P.; Svec, W. A.; Niemczyk, M. P.; Prodi, L.; Goszyola, D. In *Dynamics and Mechanics of Photoinduced Electron Transfer and Related Phenomena*; Mataga, N., Okada, T., Masuhara, H., Eds.; Elsevier: New York, 1992; p 87.
- (53) Wiederrecht, G. P.; Niemczyk, M. P.; Svec, W. A.; Wasielewski, M. R. *J. Am. Chem. Soc.* **1996**, *118*, 81.
- (54) Dielectric constants of E7 are 19.0 and 6.2 for parallel and perpendicular orientations, respectively.
- (55) Hasharoni, K.; Levanon, H. *J. Phys. Chem.* **1995**, *99*, 4875.
- (56) (a) Hasharoni, K.; Levanon, H.; von Gersdorff, J.; Kurreck, H.; Möbius, K. *J. Chem. Phys.* **1993**, *98*, 2916. (b) Hasharoni, K.; Levanon, H.; Gätschmann, J.; Schubert, H.; Kurreck, H.; Möbius, K. *J. Phys. Chem.*, **1995**, *99*, 7514.
- (57) Levanon, H.; Hasharoni, K. *Prog. React. Kinet.* **1995**, *20*, 309.
- (58) Unpublished data.
- (59) The signal rise for the total intensity is expressed by a biexponential function of the delay time based on eqs 8 and 9. However, this time profile can be written to a good approximation as the single-exponential function,  $I'(t) \approx 1 - \exp(-0.3k_D t)$ . The decay profile for the ISC spectrum, on the other hand, is orientation dependent. At field positions corresponding to the X orientation, the time dependence is given by a single-exponential function,  $I'(t) \approx 1.2 \exp(-0.3k_D t) - 0.15$ . Therefore, the signal rise with  $\lambda_{ex} = 540$  nm and decay with  $\lambda_{ex} = 640$  nm are expected to have the same time constant in the model.
- (60) (a) Fujisawa, J.; Ishii, K.; Ohba, Y.; Yamauchi, S.; Fuhs, M.; Möbius, K. *J. Phys. Chem. A* **1997**, *101*, 5869. (b) Ishii, K.; Fujisawa, J.; Ohba, Y.; Yamauchi, S. *J. Am. Chem. Soc.* **1996**, *118*, 13079.
- (61) Mizuochi, N.; Ohba, Y.; Yamauchi, S. *J. Phys. Chem. A* **1997**, *101*, 5966.
- (62) Corvaja, C.; Maggini, M.; Prato, M.; Scorrano, G.; Venzin, M. *J. Am. Chem. Soc.* **1995**, *117*, 8857.
- (63) Corvaja, C.; Maggini, M.; Ruzzi, M.; Scorrano, G.; Toffoletti, A. *Appl. Magn. Reson.* **1997**, *12*, 477.
- (64) Bencini, A.; Gatteschi, D. In *EPR of Exchange Coupled Systems*; Springer-Verlag: Berlin, 1990.
- (65) The  $g$ -factors of the free base triplet and the copper ground state doublet were obtained from simulation of the corresponding spectra of the monomers.